Mathew et al., https://doi.org/10.1083/jcb.201612018

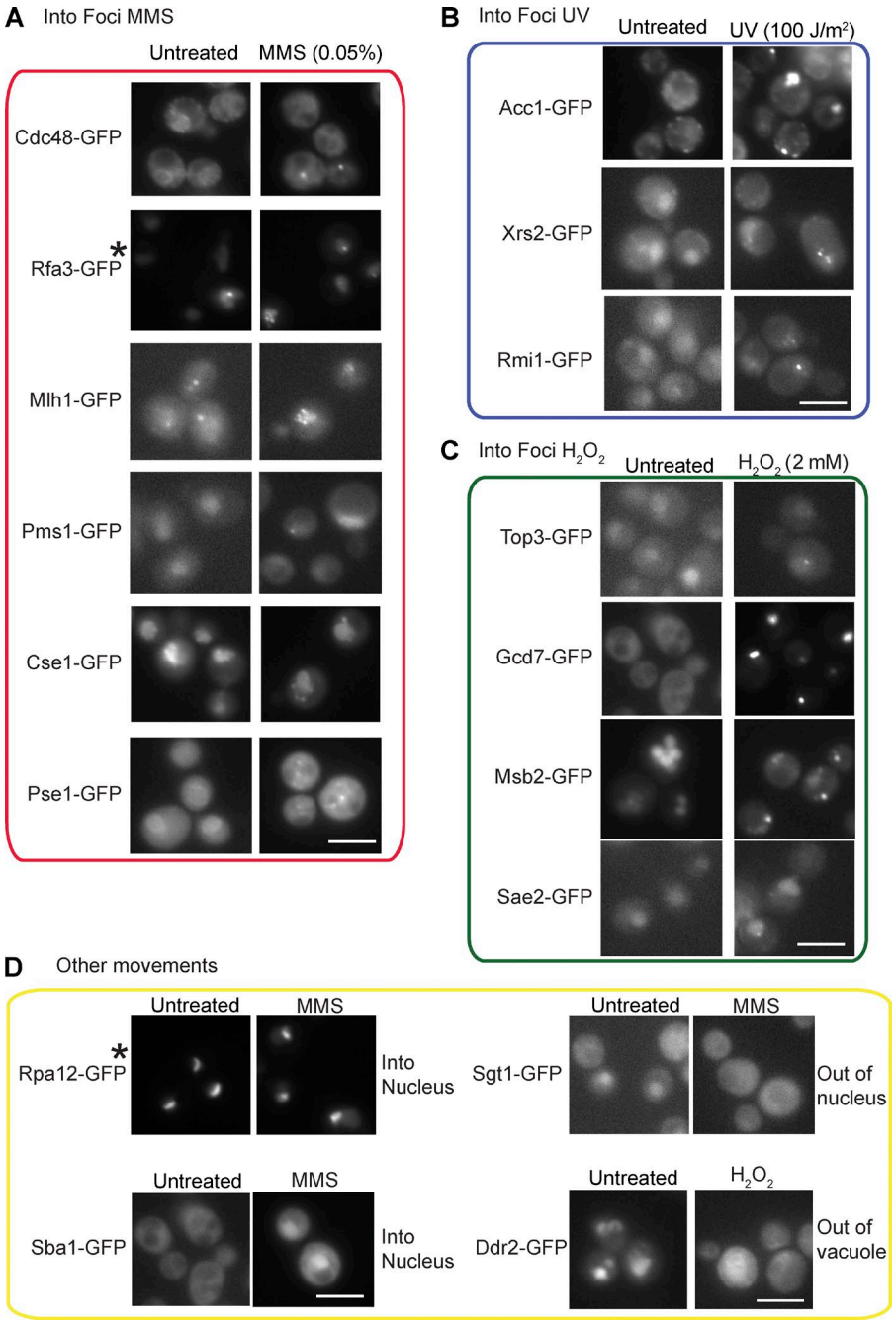

Figure S1. **Novel protein relocalization behaviors in the CIN miniarray screen.** (A–C) Movement types are grouped as indicated: (A) MMS-induced foci (red box), (B) UV-induced foci (blue box), and (C) H_2O_2-induced foci (green box). (D) Nonfoci movements as shown (yellow box). Only those not reported by Tkach et al. (2012) and a single condition is shown for clarity; however, proteins may move in response to multiple stresses. For a complete list, see Table S1. In each case, the untreated localization is on the left, and the indicated treatment is shown on the right. Hsh155-GFP relocalization is not depicted (see Fig. 1). The asterisks indicate that this is a representative of multiple members of a protein complex. In the case of Rfa3-GFP, its partners Rfa2 and Rfa1 also showed more foci in MMS (see Table S1). In the case of Rpa12-GFP, its partners Rpa14 and Rpa34 also showed observed increases in nucleoplasm versus nucleolar fluorescence in MMS. The Rpa12-GFP observation was confirmed by measuring nucleoplasmic fluorescence by colocalizing with HTA2-mCherry and quantifying the GFP signal in the nonnucleolar nuclear area (n = 17; P = 0.016; t test). Bars, 5 µm.

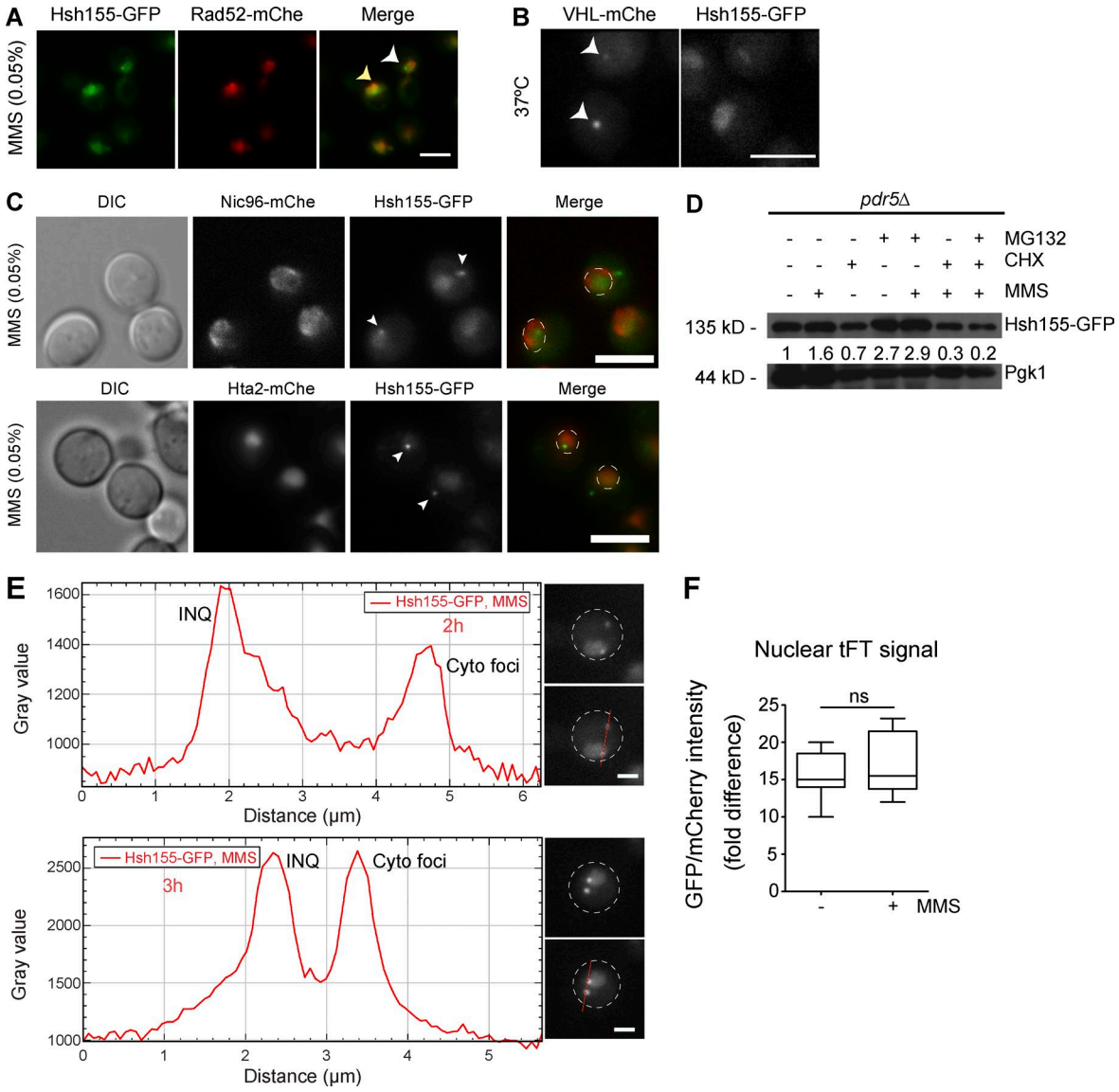

Figure S2. **Characterization of Hsh155 relocalization under stress.** (A) Hsh155-GFP foci (white arrowhead) do not colocalize with Rad52-mCherry foci (yellow arrowhead) after 2 h of MMS treatment. (B) Hsh155 do not form foci with heat stress at 37°C, whereas a VHL control does (arrowheads). (C) Localization (white arrowheads in merge) of Hsh155-GFP in nucleus and cytoplasm; nuclear periphery was marked with Nic96-mCherry (mChe; top), and chromatin was marked with Hta2-mCherry (bottom) in MMS. Bars, 5 µm. DIC, differential interference contrast. Dashed circles denote cell borders. (D) Hsh155 protein levels relative to Pgk1 levels (as indicated) in cells treated with MMS (0.05%) and/or CHX (200 µg/ml), MG132 (80 µM) alone, or together for 2 h. Hsh155 protein levels appear to be comparable to untreated in all treatments. (E) Line scan plots of Hsh155-GFP intensities in INQ and cytoplasmic foci (depicted by dotted red lines in representative images) at 2 (top) and 3 (bottom) h of MMS treatment. Bars, 2 µm. Representative graphs are shown in Fig. 3 C. Dashed circles denote cell borders. (F) Quantification of fold differences in Hsh155 tandem fusion to a fluorescent timer shows nonsignificant differences in lifetime between untreated and MMS-treated nucleoplasm. $n = 3$ with ≥ 30 cells each. tFT, tandem fluorescent protein timer.

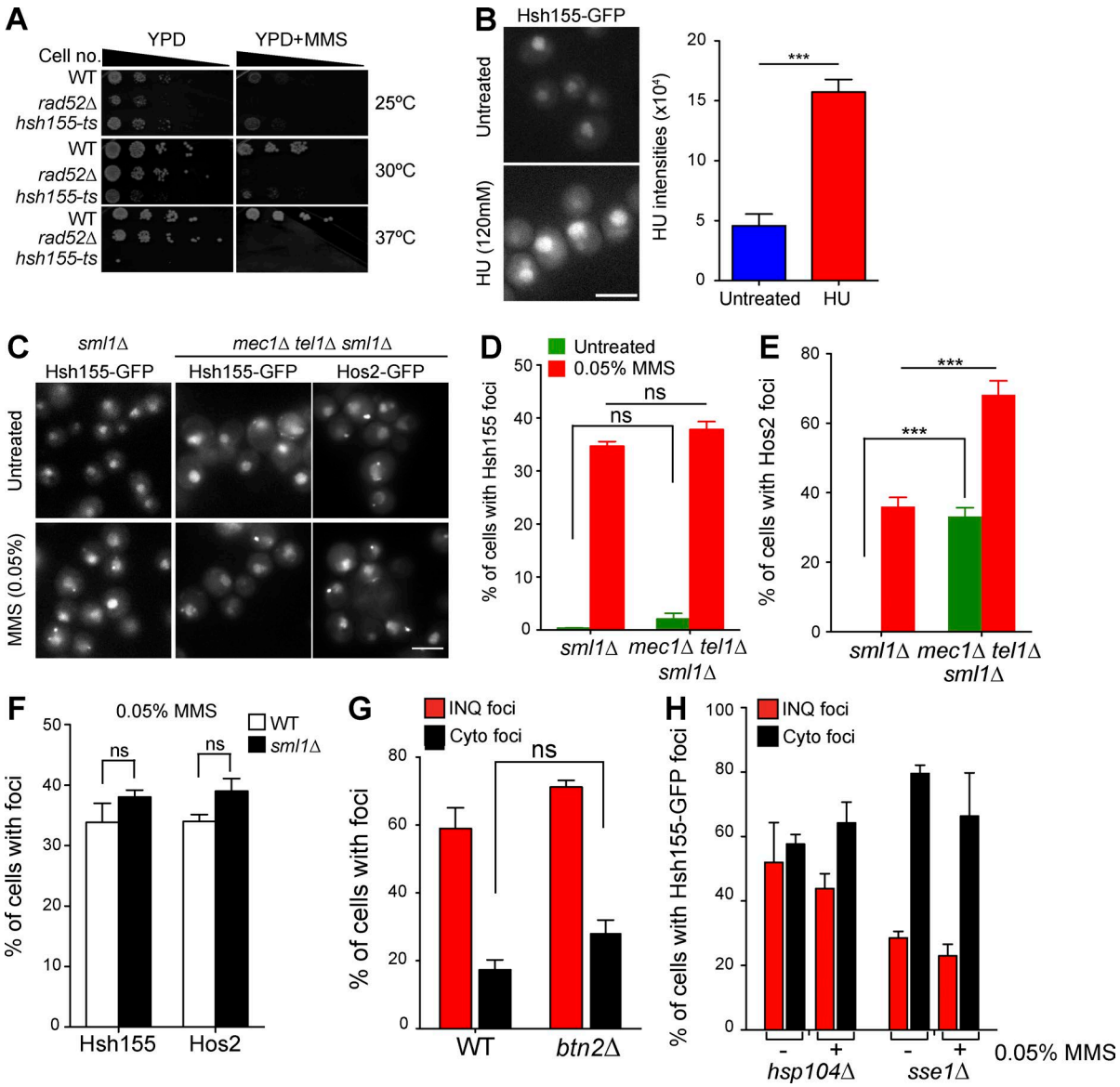

Figure S3. **Replication stress does not regulate Hsh155 foci formation and foci distribution in chaperones.** (A) *hsh155-ts* alleles are ts but not additionally MMS-sensitive compared with WT and *rad52Δ* (sensitive control) strains. Equal ODs of the indicated strains were serially diluted and spotted on YPD ± 0.01% MMS at 25°C, 30°C, and 37°C. (B) Representative images showing no foci formation but increases in Hsh155 intensities in HU-treated (120 mM; 2-h treatment) cells compared with untreated. On the right is single-cell quantifications of mean intensity of Hsh155 protein per cell as depicted in the image. Student's *t* test. (C and D) Loss of *MEC1* and *TEL1* does not influence Hsh155 localization but Hos2 aggregate formation. Bar graph (D) and representative image (C) show no significant difference in Hsh155 localization in *mec1Δtel1Δsml1Δ* in either untreated (green bars) or MMS-treated (red bars) cells compared with *sml1Δ*. (E) Loss of *MEC1* and *TEL1* influences Hos2 aggregate formation. Bar graph shows significant difference in Hos2 localization in *mec1Δtel1Δ* in both untreated (green bars) and MMS-treated cells (red bars). (F) Bar graph showing no significant difference in localization of either Hsh155 or Hos2 in *sml1Δ* control for *mec1Δtel1Δsml1Δ* mutants. Three replicates; $n > 100$; means ± SEM. (G) Effect of deleting *BTN2* on INQ and cytoplasmic foci distribution. No significant difference in both nuclear and cytoplasmic foci distribution in *btn2* mutants compared with WT. Shown are the mean values from three independent experiments ± SEM with at least 100 cells each. P-value thresholds; *, $P < 0.05$; ***, $P < 0.001$; Fisher's test. (H) Effect of deleting *HSP104* and *SSE1* on INQ and cytoplasmic foci distribution. The percentages of cells with cytoplasmic foci (black bars) increased in *hsp104* mutants in MMS and in both untreated and MMS-treated cells in *sse1* mutants. Mean values from three independent experiments ± SEM with at least 100 cells each.

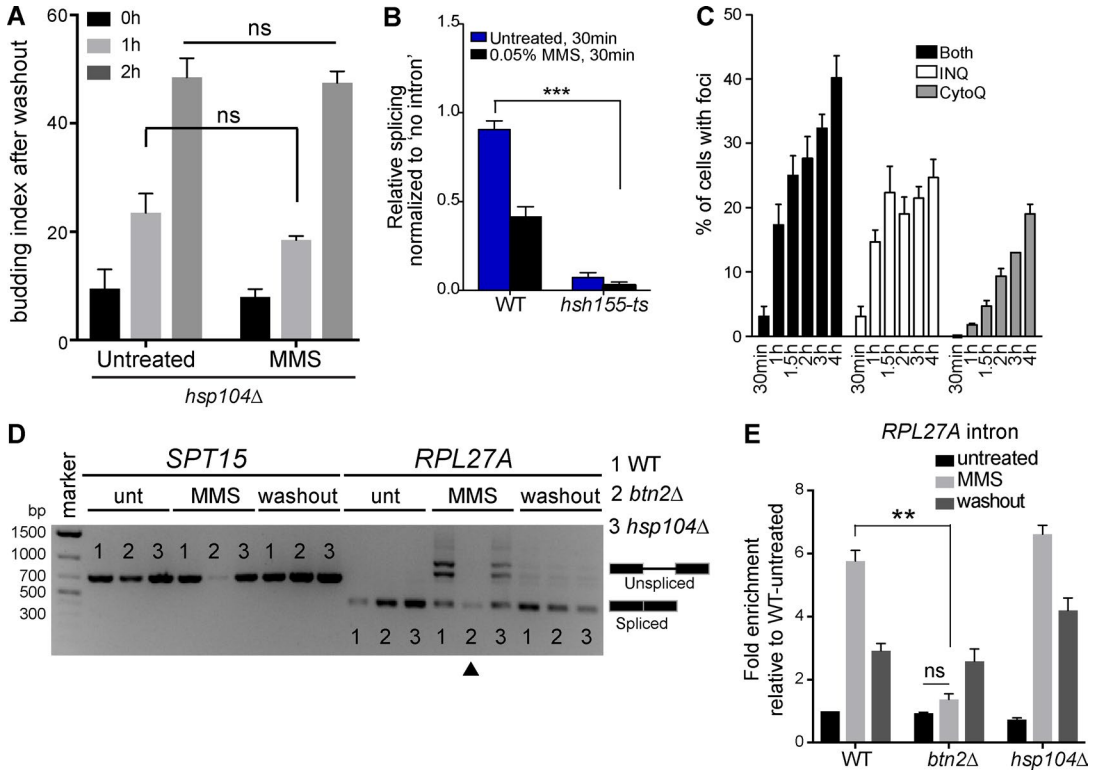

Figure S4. **Transcriptional remodeling under stress linking to PQC site targets.** (A) Quantification of the percentage of large-budded cells in both *HSP104*-deleted and WT strains synchronized and released from G1 phase with or without MMS washout. *hsp104*Δ cells showed no significant delay in rebudding overtime after MMS washout, comparable to untreated and WT cells. $n = 3$ with >30 cells each. (B) Splicing efficiency in *hsh155-ts* (used as a positive control) at 30°C compared with WT was significantly reduced with and without MMS treatment. Quantification of relative splicing in untreated (blue bars) and MMS-treated (black bars) normalized to "no intron" control. $n = 3$ with individual transformants in triplicates each. Results were compared with a *t* test. (C) Hsh155 protein aggregates at PQC sites were not formed until 1 h of MMS treatment. Percentage of cells with foci in INQ (white bars), cytoplasm (gray bars), or both (black bars) after MMS treatment at different times as indicated. No claims of significance are made. $n = 3$ with >100 cells each. (D) Hsh155 aggregate formation influenced RPG intron retention in MMS. Expression and splicing of *RPL27A* transcripts compared with intronless *SPT15* in WT, *BTN2*-, and *HSP104*-deleted strains with or without MMS and 2 h after MMS washout. cDNA PCR products representing spliced cells, and unspliced cells are indicated. MMS treatment led to intron retention in WT and *hsp104*Δ cells. Loss of *BTN2* prevented this MMS-induced intron retention (arrowhead). Unt, untreated. (E) Quantification of *RPL27A* transcript levels from the intron region in WT, *BTN2*-, and *HSP104*-deleted strains by reverse transcription–quantitative PCR normalized to *SPT15* and relative to WT untreated. As shown in D, MMS treatment led to significant intron retention in WT and *hsp104*Δ cells but not in *btn2*Δ cells. Three biological replicates; means ± SEM; asterisks show p-values of ΔΔCt levels; **, $P < 0.01$; ***, $P < 0.001$.

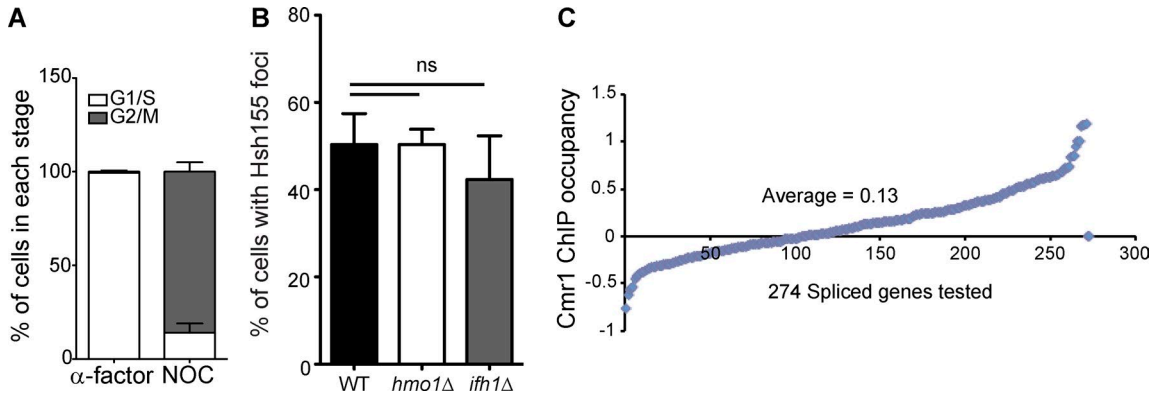

Figure S5. **TORC1 signaling influences sequestration of transcription regulators to PQC.** (A) Percentage of cells arrested in G1/S (white) and G2/M (gray) in α-factor– and nocodazole (NOC)-treated cells as judged by budding index. (B) Effect of RPG transcription regulators Hmo1 and Ifh1 on Hsh155 relocalization after MMS treatment. Three replicants; means ± SEM; $n > 100$; Fisher's test. (C) Scatter plot showing distribution of 274 spliced genes (X axis) with their corresponding Cmr1 ChIP occupancy (Y axis/$\log_2$ ratio ChIP/input). The plot indicates a highly significant and larger Cmr1 occupancy in WT cells (Jones et al., 2016) at spliced genes. Mean Cmr1 occupancy for 274 spliced genes was 0.13, and mean occupancy for all genes was 0.046. $P < 0.0001$; two-tailed Student's *t* test (for all the genes, $n = 5{,}549$, and for spliced genes, $n = 274$; compared listed in Table S4).

Table S1 is a separate Excel document showing a list of GFP-tagged CIN gene miniarray screen proteins showing localization changes after MMS, H2O2, or UV treatment.

Table S2 is a separate Excel document showing the whole-proteome abundance data after MMS treatment.

Table S3 is a separate Excel document showing the Gene Ontology enrichment for depleted proteins upon MMS treatment.

Table S4 is a separate Excel document showing a comparison of the Cmr1 ChIP occupancy data in WT cells and complete microarray expression data in *sfp1Δ* strain.

Table S5 is a separate Excel document showing yeast strains, primers, and plasmids used in this study.

Text S1 is a separate text file containing source code for the R pipeline used in FRAP analysis.

References

Jones, J.W., P. Singh, and C.K. Govind. 2016. Recruitment of Saccharomyces cerevisiae Cmr1/Ydl156w to Coding Regions Promotes Transcription Genome Wide. *PLoS One.* 11:e0148897. https://doi.org/10.1371/journal.pone.0148897

Tkach, J.M., A. Yimit, A.Y. Lee, M. Riffle, M. Costanzo, D. Jaschob, J.A. Hendry, J. Ou, J. Moffat, C. Boone, et al. 2012. Dissecting DNA damage response pathways by analysing protein localization and abundance changes during DNA replication stress. *Nat. Cell Biol.* 14:966–976. https://doi.org/10.1038/ncb2549